THE PUBLISHING HOUSE
OF THE ROMANIAN ACADEMY

PROCEEDINGS OF THE ROMANIAN ACADEMY, Series A,
Volume 19, Number 2/2018, pp. 329–336

SECOND-ORDER ANISOTROPIC DIFFUSION-BASED FRAMEWORK FOR STRUCTURAL INPAINTING

Tudor BARBU

Institute of Computer Science of the Romanian Academy
E-mail: tudor.barbu@iit.academiaromana-is.ro

Abstract. A novel structure-based image interpolation technique is proposed in this paper. It is based on a nonlinear anisotropic diffusion model that is properly constructed for the reconstruction process. A rigorous mathematical investigation of this partial differential equation (PDE) - based scheme is then performed, its well-posedness being treated. An explicit finite difference-based numerical approximation scheme that is consistent to the second-order PDE model and converges to its weak solution is developed next. The successful inpainting experiments and method comparison prove the effectiveness of the considered diffusion-based approach.

Key words: structural inpainting, nonlinear anisotropic diffusion, second-order PDE model, well-posedness analysis, finite-difference method, numerical approximation scheme.

1. INTRODUCTION

The digital *image inpainting* task represents one of the fundamental problems in the image processing domain. It is known also as *image completion*, and represents the process of automatic reconstruction of the missing parts of deteriorated images by employing the information obtained from the surrounding regions. Therefore, it represents an interpolation problem, so it is also named *image interpolation*. Also, the term *inpainting* is an ancient very old term that originates from the art restoration [1].

Image interpolation has many applications in various important image processing fields. Let us mention here the damaged painting reconstruction, photo and movie restoration, image and video object removal / replacing, solving the disocclusion, zooming and super-resolution, estimating the scene behind an obscuring foreground, and image de/compression and coding [1].

While some image completion techniques can reconstruct only structures, and other methods inpaint only image textures, there exist approaches that recover both of them. Some texture-based inpainting techniques are based on the texture synthesis [2, 3], while other schemes represent exemplar-based approaches [4, 5].

The structural inpainting techniques use energy-based and PDE-based models to reconstruct the missing or highly damaged regions. The energy-based, or variational, models inpaint the image by solving a minimization problem involving an energy functional. The most influential variational interpolation approaches include Mumford-Shah Inpainting [6], the model of Masnou and Morel [7], and Total Variation Inpainting [1, 8]. Some improved versions of total variation inpainting that have been developed in the last years include TV Inpainting with Split Bregman [9], Blind Inpainting using l_0 and TV Regularization [10] and TV Inpainting with Primal-Dual Active Set (PDAS) method [11].

Also, many second and higher order PDE-based inpainting models have been developed in the last decades. An influential anisotropic diffusion model for image inpainting is that introduced by Bertalmio *et al*. in [12]. Unlike second-order diffusion models that follow variational principles, the high-order PDE inpainting approaches are not derived from some variational schemes, being directly given as evolutionary differential equations. They include the third-order interpolation models, such as Curvature-driven Diffusion (CDD) Inpainting [1, 13], and the fourth-order PDE-based completion schemes, like Cahn-Hillard Inpainting, TVH^{-1} Inpainting and LCIS Inpainting [1, 13].

Some interpolation methods that perform simultaneous structure and texture image inpainting have also been developed in the last years. They combine the PDE variational models to texture synthesis based approaches [14, 15].

We have also developed numerous variational and PDE-based inpainting technique in our past works [16–18]. In this article we consider a novel second-order PDE-based interpolation approach based on a nonlinear anisotropic diffusion-based model. The proposed PDE model is described in the following section and a rigorous mathematical treatment is performed on it in the third section, its well-posedness being demonstrated.

A robust numerical approximation scheme that is consistent to this anisotropic diffusion model and converges fast to its solution is developed, by using the finite difference method, in the fourth section. Our succesful inpainting experiments and method comparison are described in the fifth section. The work ends with a section of final conclusions.

2. NONLINEAR ANISOTROPIC DIFFUSION-BASED INTERPOLATION MODEL

Given an observed image that contains highly damaged or missing regions, it can be represented as a partial two-dimension function that is defined only outside of those zones, $u_0 : \Omega \setminus \Gamma \to R$, where the image domain $\Omega \subseteq R^2$ and Γ represents the missing part of the image, being expressed as a set of pixel coordinates. Therefore, the image that is evolving during the inpainting process has the form $u : \Omega \to R$, $u\big|_{\Omega \setminus \Gamma} = u_0$. We consider the following nonlinear second-order anisotropic diffusion model with boundary conditions that recovers the original image from the observed image:

$$\begin{cases} \dfrac{\partial u}{\partial t} - \psi^u\left(\|\nabla u\|\right)\nabla \cdot \left(\varphi_u\left(\|\nabla u\|\right)\nabla u\right) + \lambda\left(1 - 1_\Gamma\right)\left(u - u_0\right) = 0, \quad \forall (x, y) \in \Omega \\ u(x, y, 0) = u_0(x, y), \quad \forall (x, y) \in \Omega \\ u(t, x, y) = 0, \quad \forall (x, y) \in \partial\Omega \end{cases} \tag{2.1}$$

where $\lambda \in (0, 1]$. This parabolic PDE-based model uses an *inpainting mask* that is provided by the next characteristic function:

$$1_\Gamma(x, y) = \begin{cases} 1, & \text{if } (x, y) \in \Gamma \\ 0, & \text{if } (x, y) \notin \Gamma. \end{cases} \tag{2.2}$$

The first function of the anisotropic diffusion model provided by (2.1) is constructed in the following form:

$$\begin{cases} \psi : (0, \infty) \to (0, \infty) \\ \psi^u(s) = \gamma\left(\alpha s^r + \beta\right)^{\frac{1}{r+1}}, \end{cases} \tag{2.3}$$

where the parameters $\alpha, \gamma \in (0, 3]$, $\beta \in (0, 3.5]$, $r \in (0, 2]$. The next diffusivity function is proposed for the PDE model:

$$\begin{aligned} &\varphi_u : [0, \infty) \to [0, \infty) \\ &\varphi_u(s) = \delta\left(\frac{\eta(u)}{\xi s^k + \nu \log 10\left(\eta(u)\right)}\right)^{\frac{1}{k+1}}, \end{aligned} \tag{2.4}$$

where $\delta \in (0,2)$, $\xi \in (1,5]$, $\nu \in (0,1)$ and $k \in \{1,2,3,4\}$. The conductance parameter in (2.4) is modeled as:

$$\eta\left(u(x, y, t)\right) = \left|\varepsilon\mu\left(\|\nabla u\|\right) + \zeta t\right|, \tag{2.5}$$

where $\varepsilon > 1$, $\zeta \in (0,1)$ and $\mu(\ )$ is the averaging operator.

The anisotropic diffusion-based framework given by (2.1) – (2.5) performs the inpainting by directing the diffusion mostly to the missing image regions and reducing it outside of these zones. The diffusivity function (2.4) is properly constructed, satisfying the main conditions required by a successful diffusion process [19].

Thus, the function φ_u is positive, since $\varphi_u(s) > 0, \forall s \in (0,\infty)$. It is also monotonically decreasing, since $\varphi_u(s_1) = \delta\left(\frac{\eta(u)}{\xi {s_1}^k + \nu \log 10(\eta(u))}\right)^{\frac{1}{k+1}} \geq \varphi_u(s_2) = \delta\left(\frac{\eta(u)}{\xi {s_2}^k + \nu \log 10(\eta(u))}\right)^{\frac{1}{k+1}}$, $\forall s_1 \leq s_2$. Also, this function converges to zero when s goes to infinity: $\lim_{s\to\infty} \varphi_u(s) = 0$. The component based on the other function, $\psi^u(\|\nabla u\|)$, is controlling the speed of the image diffusion process.

The inpainted image is determined by solving the described nonlinear differential model. Therefore, in the following section we treat its well-posedness, investigating the existence and uniqueness of a weak solution that would represent the optimal image interpolation. A numerical approximation of that solution is performed in the fourth section.

3. A MATHEMATICAL TREATMENT OF THE PROPOSED PDE MODEL

The mathematical validity of the considered nonlinear second-order PDE model is investigated in this section. Thus, we demonstrate the well-posedness of this anisotropic diffusion model, meaning the existence and uniqueness of a weak solution for it, under some certain assumptions.

So, we have:

$$\psi^u(\|\nabla u\|^2)\nabla\cdot(\varphi_u(\|\nabla u\|^2)\nabla u) = div(\psi^u(\|\nabla u\|^2)\varphi_u(\|\nabla u\|^2)\nabla u) - 2\varphi_u(\|\nabla u\|^2)\psi^u{}'(\|\nabla u\|^2)|\nabla u|^2\Delta u \quad (2.6)$$

Let us set:

$$g(s) = 2\int_0^s \varphi_u(z)\psi^u{}'(z)z^2 dt, \forall s > 0 \quad (2.7)$$

Therefore, we get:

$$2\varphi_u(\|\nabla u\|^2)\psi^u{}'(\|\nabla u\|^2)|\nabla u|^2\Delta u = div(g(\|\nabla u\|^2)\nabla u) - 2g'(\|\nabla u\|^2)|\nabla u|^2 \quad (2.8)$$

Finally, by (2.7) one obtains:

$$\psi^u(\|\nabla u\|^2)div(\varphi_u(\|\nabla u\|^2)\nabla u) = div((\psi^u(\|\nabla u\|^2)\varphi_u(\|\nabla u\|^2) - g(\|\nabla u\|^2))\nabla u) - 4\varphi_u(\|\nabla u\|^2)\psi^u{}'(\|\nabla u\|^2)\|\nabla u\|^2 \quad (2.9)$$

Hence we may re-write the partial differential equation is (2.1) as following:

$$\frac{\partial u}{\partial t} = div((\psi^u(\|\nabla u\|^2)\varphi_u(\|\nabla u\|^2) - g(\|\nabla u\|^2))\nabla u) + 4\varphi_u(\|\nabla u\|^2)\psi^u{}'(\|\nabla u\|^2)\|\nabla u\|^2 \quad (2.10)$$

We have to assume that the function $\psi^u(s^2)\varphi_u(s^2) - g(s^2)$ is convex and $\psi^u(s^2)\varphi_u(s^2) - g(s^2) \geq \rho > 0, \forall s > 0$, where ρ is a constant. A function u is said to be a weak or variational solution to (2.10) if it satisfies:

$$\frac{\partial}{\partial t}\int_\Omega u(t,x,y)\chi(x,y)dxdy + \int_\Omega (\psi^u(\|\nabla u\|^2)\varphi_u(\|\nabla u\|^2) - g(\|\nabla u\|^2))\nabla u\cdot\nabla\chi\, dxdy \quad (2.11)$$

$$-4\int_{\Omega}\varphi_u\left(\|\nabla u\|^2\right)\psi'\left(\|\nabla u\|^2\right)\|\nabla u\|\chi dxdy=0$$

for $(x, y)\in C^{\infty}(\Omega)$, $u \in L^2\left(0, T; H_0^1(\Omega)\right)$, and $\frac{\partial u}{\partial t}\in L^2\left(0, T; H^{-1}(\Omega)\right)$, where $H_0^1(\Omega)$ is a Sobolev space and $H^{-1}(\Omega)$ is its dual.

We fix $v \in L^2\left(0, T; H_0^1(\Omega)\right)$, then consider the next equation:

$$\begin{cases}\frac{\partial u}{\partial t}-div\left(\left(\psi^u\left(\|\nabla u\|^2\right)\varphi_u\left(\|\nabla u\|^2\right)-g\left(\|\nabla u\|^2\right)\right)\nabla u\right)=4\varphi_v\left(\|\nabla v\|^2\right)\psi^{v\prime}\left(\|\nabla v\|^2\right)\|\nabla v\|^2\\ u(0, x, y)=u_0(x, y)\\ u(t, x, y)=0 \text{ on } (0, T)\times\partial\Omega\end{cases} \tag{2.12}$$

The problem (2.12) is parabolic in *u* and so it has a unique solution satisfying $u \in L^2\left(0, T; H_0^1(\Omega)\right)$ and $\frac{\partial u}{\partial t}\in L^2\left(0, T; H^{-1}(\Omega)\right)$. Then one proves that on a small interval the operator $v \to u$ is a contraction in $L^2\left(0, T; H_0^1(\Omega)\right)$ and, by applying the Banach's fixed point theorem [20], demonstrates that (2.10), with $u_0 \in L^2(\Omega)$ has an unique solution on some interval $(0, T)$. Thus, the proposed nonlinear diffusion model is well-posed.

4. NUMERICAL APPROXIMATION ALGORITHM

The nonlinear anisotropic diffusion model proposed and analysed in the previous sections can be solved numerically using an iterative discretization algorithm that approximates its solution representing the inpainted image. We assume a space grid size of *h* and a time step size of Δt and quantize the time and space coordinates as following:

$$x = ih,\ y = jh,\ t = n\Delta t,\ i \in \{1,..., I\},\ j \in \{1,..., J\},\ n \in \{0,..., N\} \tag{2.13}$$

where $[Ih \times Jh]$ is the size of the image support.

A robust discretization of the PDE model (2.1) is then performed by using the finite difference method [19, 21]. First, the PDE in (2.1) leads to

$$\frac{\partial u}{\partial t} = \psi^u(\|\nabla u\|)\left(\frac{\partial}{\partial x}\left(\varphi_u(\|\nabla u\|)u_x\right)+\frac{\partial}{\partial y}\left(\varphi_u(\|\nabla u\|)u_y\right)\right)-\lambda(1-1_\Gamma)(u-u_0) \tag{2.14}$$

Then, a finite difference-based numerical approximation is applied on (2.14). The gradient magnitude is approximated by using central differences [21], as follows:

$$\|u_{i,j}\| \approx \sqrt{\left(\frac{u_{i+h,j}-u_{i-h,j}}{2h}\right)^2+\left(\frac{u_{i,j+h}-u_{i,j-h}}{2h}\right)^2} \tag{2.15}$$

We then compute $\psi_{i,j}=\psi^u\left(\|u_{i,j}\|\right)$ and $\varphi_{i,j}=\varphi_u\left(\|u_{i,j}\|\right)$, by applying (2.3), (2.4) and (2.15). The component $\frac{\partial}{\partial x}\left(\varphi_u(\|\nabla u\|)u_x\right)$ gets the spatial discretization $\varphi_{i+\frac{h}{2},j}\left(u_{i+h,j}-u_{i,j}\right)-\varphi_{i-\frac{h}{2},j}\left(u_{i,j}-u_{i-h,j}\right)$ and the component $\frac{\partial}{\partial y}\left(\varphi_u(\|\nabla u\|)u_y\right)$ is approximated as $\varphi_{i,j+\frac{h}{2}}\left(u_{i,j+h}-u_{i,j}\right)-\varphi_{i,j-\frac{h}{2}}\left(u_{i,j}-u_{i,j-h}\right)$, where:

$$\varphi_{i\pm\frac{h}{2},j} = \frac{\varphi_{i\pm h,j} + \varphi_{i,j}}{2}, \varphi_{i,j\pm\frac{h}{2}} = \frac{\varphi_{i,j\pm h} + \varphi_{i,j}}{2} \tag{2.16}$$

Then, by using forward difference for time derivative [21], one obtains the following discretization for (2.14):

$$\begin{aligned}\frac{u_{i,j}^{n+\Delta t} - u_{i,j}^{n}}{\Delta t} &= \psi_{i,j}\left(\varphi_{i+\frac{h}{2},j}\left(u_{i+h,j}^{n} - u_{i,j}^{n}\right) - \varphi_{i-\frac{h}{2},j}\left(u_{i,j}^{n} - u_{i-h,j}^{n}\right) + \varphi_{i,j+\frac{h}{2}}\left(u_{i,j+h}^{n} - u_{i,j}^{n}\right) - \varphi_{i,j-\frac{h}{2}}\left(u_{i,j}^{n} - u_{i,j-h}^{n}\right)\right) \\ &- \lambda\left(1 - 1_{\Gamma}\right)\left(u_{i,j}^{n} - u_{i,j}^{0}\right)\end{aligned} \tag{2.17}$$

We may consider the parameter values $\Delta t = h = 1$. The implicit approximation (2.17) leads to the next explicit iterative numerical approximation scheme:

$$\begin{aligned}u_{i,j}^{n+1} &= u_{i,j}^{n}\left(1 - \lambda\left(1 - 1_{\Gamma}\right) + \psi_{i,j}\left(\varphi_{i+\frac{1}{2},j} + \varphi_{i-\frac{1}{2},j} + \varphi_{i,j+\frac{1}{2}} + \varphi_{i,j-\frac{1}{2}}\right)\right) + u_{i+1,j}^{n}\psi_{i,j}\varphi_{i+\frac{1}{2},j} + u_{i-1,j}^{n}\psi_{i,j}\varphi_{i-\frac{1}{2},j} + \\ &+ u_{i,j+1}^{n}\psi_{i,j}\varphi_{i,j+\frac{1}{2}} + u_{i,j-1}^{n}\psi_{i,j}\varphi_{i,j-\frac{1}{2}} + u_{i,j}^{0}\lambda\left(1 - 1_{\Gamma}\right)\end{aligned} \tag{2.18}$$

with $u_{0,j}^{n} = u_{1,j}^{n}, u_{I,j}^{n} = u_{I+1,j}^{n}, u_{i,0}^{n} = u_{i,1}^{n}, u_{i,J}^{n} = u_{i,J+1}^{n}$. The numerical approximation scheme (2.18) is consistent to the anisotropic diffusion model (2.1) and converges fast to its solution representing the recovered image.

5. EXPERIMENTS AND METHOD COMPARISON

The proposed nonlinear PDE-based inpainting approach has been tested on hundreds images affected by missing or highly damaged parts, satisfactory results being achieved. Some of the image collections used in the experiments are the volumes of the USC - SIPI database. The performance of our technique has been assessed using image similarity measures such as PSNR (peak signal to noise ratio), SNR (signal to noise ratio) and MSE (mean-squared error) [22]. We have determined an optimal set of values for the parameters in (2.1) – (2.5), by using the trial and error method with these measures. These values providing an optimal image reconstruction are the following:

$$\lambda = 0.7, \gamma = 0.6, \alpha = 1.2, \beta = 1.7, r = 0.45, \delta = 0.5, \xi = 3.5, \nu = 0.4, k = 2, \varepsilon = 1.7, \zeta = 0.3 \tag{2.19}$$

Our inpainting technique is characterized by a quite low running time, since the iterative discretization algorithm (2.18) converges fast to the optimal reconstruction. The number of its steps, *N*, is rather low, but it is also influenced by the size of the missing (damaged) part of the processed image, and also by the amount of image noise, increasing proportionally with these factors.

Also, the diffusion-based completion method developed by us interpolates successfully the deteriorated images while preserving their edges, corners and other essential features. It performs efficiently in noisy conditions too, reducing the amount of additive Gaussian noise and the unintended effects. See some inpainting results achieved by our technique in both normal and noisy conditions (Gaussian noise with μ = 0.21 and *var* = 0.02) in Fig.1. But, while our approach provides an effective structure-based inpainting, it performs considerably weaker in the textural inpainting case.

Method comparison have been also performed. The anisotropic diffusion-based reconstruction technique described here has been compared to some well-known existing PDE-based and variational interpolation schemes. Thus, it clearly outperforms second-order PDE models, such as Harmonic Inpainting [1], TV Inpainting and other completion schemes derived from diffusion-based denoising methods, achieving higher PSNR and lower MSE values, and obtains comparable good results to fourth-order PDE inpainting schemes, like TV – H^{-1} Inpainting.

See some method comparison results in Table 1 and Fig. 2. While TV – H^{-1} Inpainting achieves slightly better average values for these performance metrics, the AD (anisotropic diffusion) scheme described here converges much faster and has a considerably lower execution time. Our inpainting approach reaches the optimal image completion in much fewer iterations (t = 45) than other PDE-based algorithms, especially the

TV-based ones requiring around 1 000 steps, as one can see in Fig. 2 that displays inpainting results produced by several methods on $[512 \times 512]$ *Barbara* image affected by 2 missing regions (black hand-written texts).

a) Original *Lenna* image

b) Image corrupted by missing zone

c) Inpainting result – $N = 29$

d) Gaussian noise + missing part

e) Inpainting in noisy conditions: $N = 39$

Fig. 1 – Inpainting output produced by the proposed AD algorithm in normal and noisy conditions.

Table 1

Method comparison: average PSNR and MSE values

Inpainting technique	**Peak Signal to Noise Ratio (PSNR)**	**Mean Squared Error (MSE)**
The proposed AD Inpainting	36.1338 (dB)	15.8380
Harmonic Inpainting	29.6887 (dB)	69.8576
Total Variation Inpainting	34.2561 (dB)	24.4047
TV – H^{-1} Inpainting	36.3805 (dB)	14.9634

a) Original image

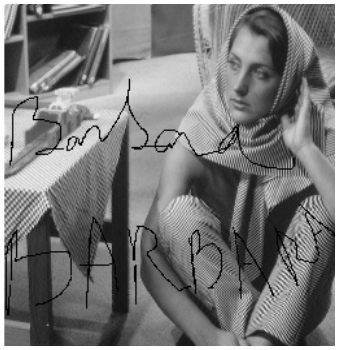

b) Image affected by missing parts

c) This AD inpainting ($t = 45$)

d) harmonic inpainting ($t = 50$)

e) TV inpainting ($t = 850$)

f) TV – H^{-1} inpainting ($t = 1\ 500$)

Fig. 2 – Interpolation results achieved by several PDE-based inpainting models.

6. CONCLUSIONS

A novel effective non-texture PDE-based inpainting technique has been proposed in this work. It is based on a nonlinear second-order anisotropic diffusion model that represents the main contribution of this research paper.

The proposed parabolic model is based on two properly constructed diffusivity functions and a mask that corresponds to the missing (or highly damaged) part of the processed image. The interpolation framework inpaints successfully the image by directing the speedy diffusion process to that missing part, while preserving the boundaries and other important details.

The rigorous mathematical investigation on its validity, representing another contribution of this work, has demonstrated the well-posedness of the anisotropic diffusion scheme that admits a unique and weak solution under some certain assumptions. An explicit iterative finite difference method-based numerical approximation scheme that is consistent to the PDE model and converges fast to its variational solution has also been developed.

Our successful image reconstructions experiments and method comparison show the effectiveness of the proposed method. It works satisfactory in noisy conditions and performs successfully any structural inpainting task, but provides much weaker texture inpainting results, given its non-texture character. It also outperforms many state of the art PDE-based structure inpainting techniques, providing better image reconstruction results and converging much faster. As part of our future research, we intend to further improve the anisotropic diffusion-based framework, so that to become able to inpaint properly image textures also.

ACNOWLEDGEMENTS

This research has been mainly supported from the contract-based project PN-III-P4-ID-PCE-2016-0011, financed by UEFISCDI Romania.

REFERENCES

1. C. B. SCHONLIEB, *Partial Differential Equation Methods for Image Inpainting*, Vol. **29**, Cambridge University Press, 2015.
2. A. A. EFROS, T. K. LEUNG, *Texture synthesis by non-parametric sampling*, Proceedings of the International Conference on Computer Vision, **2**, pp. 1033–1038, 1999.
3. H. IGEHY, L. PEREIRA, *Image replacement through texture synthesis*, Proceedings of the International Conference on Image Processing, **3**, pp. 186–189, 1997.
4. A. CRIMINISI, P. PEREZ, K. TOYAMA, *Region filling and object removal by exemplar-based image inpainting*, IEEE Transactions on Image Processing, **13**, *9*, pp. 1200–1212, 2004.
5. V. CASELLES, *Examplar-based image inpainting and application*, SIAM News 44 (10), December 2011.
6. S. ESEDOGLU, J. SHEN, *Digital inpainting based on the Mumford-Shah Euler image model*, European Journal of Applied Mathematics, 2002.
7. S. MASNOU, J. MOREL, *Level lines based disocclusion*, Proceedings of 5th IEEE Int. Conf. Image Processing, Chicago, IL, 1998, pp. 259–263.
8. T. F. CHAN and J. SHEN, *Morphologically invariant PDE inpaintings*, UCLA CAM Report, pp. 1–15, 2001.
9. P. GETREUER, *Total Variation Inpainting using Split Bregman*, Image Processing On Line, 2, pp. 147–157, 2012.
10. M. V. AFONSO, J. M. R. SANCHES, *Blind Inpainting Using l_0 and Total Variation Regularization*, IEEE Transactions on Image Processing, **24**, *7*, pp. 2239–2253, 2015.
11. M. NERI, E. R. ZARA, *Total variation-based image inpainting and denoising using a primal-dual active set method*, Philippine Science Letters, **7**, *1*, pp. 97–103, 2014.
12. M. BERTALMIO, G. SAPIRO, V. CASELLES, C. BALLESTER, *Image inpainting*, Proc. ACM Conf. Comp. Graphics (SIGGRAPH), New Orleans, LU, July 2000, pp. 417–424.
13. B. SONG, *Topics in Variational PDE Image Segmentation, Inpainting and Denoising*, University of California, 2003.
14. M. BERTALMIO, L. VESE, G. SAPIRO, S. OSHER, *Simultaneous structure and texture image inpainting*, IEEE Transactions on Image Processing, **12**, *8*, pp. 882–889, 2003.
15. M. ELAD, J. L. STARCK, P. QUERRE, D. L. DONOHO, *Simultaneous cartoon and texture image inpainting using morphological component analysis (MCA)*, Applied and Computational Harmonic Analysis, **19**, *3*, pp. 340–358, 2005.
16. T. BARBU, *Variational image inpainting technique based on nonlinear second-order diffusions*, Computers & Electrical Engineering, **54**, pp. 345–353, 2016.

17. T. BARBU, *Hybrid Image Interpolation Technique based on Nonlinear Second and Fourth-order Diffusions*, Proceedings of the 13th International Symposium on Signals, Circuits and Systems (ISSCS'17), Iasi, Romania, July 13–14, 2017, pp. 1–5.
18. T. BARBU, *Structural Image Interpolation using a Nonlinear Second-order Hyperbolic PDE-based Model*, Proceedings of the 6th IEEE International Conference on e-Health and Bioengineering (EHB 2017), Sinaia, Romania, 22–24 June 2017, pp. 5–8.
19. J. WEICKERT, *Anisotropic Diffusion in Image Processing*, European Consortium for Mathematics in Industry. B. G. Teubner, Stuttgart, Germany, 1998.
20. V. BARBU, *Nonlinear Differential Equations of Monoton Types in Banach Spaces*, Springer, 2010.
21. P. JOHNSON, *Finite Difference for PDEs*, School of Mathematics, University of Manchester, Semester I, 2008.
22. E. SILVA, K.A. PANETTA, S.S. AGAIAN, *Quantify similarity with measurement of enhancement by entropy*, Proceedings: Mobile Multimedia / Image Processing for Security Applications, SPIE Security Symposium 2007, **6579**, April 2007, pp. 3–14.

Received December 29, 2017